Proc. Natl. Acad. Sci. USA
Vol. 89, pp. 7586–7590, August 1992
Biochemistry

Antiparallel side-by-side dimeric motif for sequence-specific recognition in the minor groove of DNA by the designed peptide 1-methylimidazole-2-carboxamide netropsin

MILAN MRKSICH*, WARREN S. WADE*, TAMMY J. DWYER†, BERNHARD H. GEIERSTANGER†, DAVID E. WEMMER†, AND PETER B. DERVAN*

*Division of Chemistry and Chemical Engineering, California Institute of Technology, Pasadena, CA 91125; and †Department of Chemistry, University of California, Berkeley, CA 94720

Contributed by Peter B. Dervan, May 6, 1992

ABSTRACT **The designed peptide 1-methylimidazole-2-carboxamide netropsin (2-ImN) binds specifically to the sequence 5′-TGACT-3′. Direct evidence from NMR spectroscopy is presented that this synthetic ligand binds DNA as a 2:1 complex, which reveals that the structure is an antiparallel dimer in the minor groove of DNA. This is in contrast to the 1:1 complexes usually seen with most crescent-shaped minor groove binding molecules targeted toward A+T-rich tracts but reminiscent of a dimeric motif found for distamycin at high concentrations. These results suggest that sequence-dependent groove width may play an important role in allowing an expanded set of DNA binding motifs for synthetic peptides.**

The natural products netropsin and distamycin A are crescent shaped di- and tripeptides, respectively, that bind in the minor groove of DNA at sites of four or five successive A·T base pairs (1–8). The structures of a number of peptide–DNA complexes have been determined by x-ray diffraction (4–6) and NMR spectroscopy (7, 8). Analysis of these structures has led to the conclusion that hydrogen bonding, van der Waals contacts, and electrostatics all contribute to the binding affinity and specificity. The minor groove of sequences containing A·T base pairs is deeper than that of G·C pair sequences due to the absence of the amino group of guanine. It has been found that the width of the minor groove of some of these A+T-rich sequences is narrower than standard B-DNA (9). The two or three *N*-methylpyrrole-carboxamides twist in a screw sense to match the walls of the minor groove, giving a favorable shape complementarity for the ligand (4–6).

Although there has been some encouraging success with regard to the design and synthesis of peptide analogs that bind larger sequences of pure A+T-rich double-stranded DNA (10–14), there has not been corresponding success in the development of well-understood G·C recognition for targets with mixed A·T and G·C sequences (15–17). Attachment of pyridine-2-carboxamide to the amino terminus of the dipeptide bis-*N*-methylpyrrolecarboxamide affords the tripeptide pyridine-2-carboxamide netropsin (2-PyN), which binds specifically the sequence 5′-TGACT-3′ as well as the family of 5′-(A·T)$_5$-3′ sequences (18, 19). Although this molecule was designed to bind sequences of the type 5′-(G·C)(A·T)$_3$-3′ in a single orientation preference, affinity cleaving experiments revealed that the 2-PyN–5′-TGACT-3′ complex is composed of two equivalent orientations (19, 20). Models of a 1:1 ligand–DNA complex seemed inadequate for rationalizing either the approximate twofold symmetry of the complex or the recognition of G·C base pairs in both the second and fourth positions of the 5′-TGACT-3′ site (18). In an effort to explore the structural limitations for 2-PyN, pyridine has been replaced by *N*-methylimidazole to afford 1-methylimidazole-2-carboxamide netropsin (2-ImN) (19). From footprinting analysis, this molecule binds the sequence 5′-TGACT-3′ more strongly than 5′-(A·T)$_5$-3′ tracts (19, 20). In addition, from affinity cleaving, the complex of 2-ImN–5′-TGACT-3′ is composed of two equivalent orientations (19, 20).

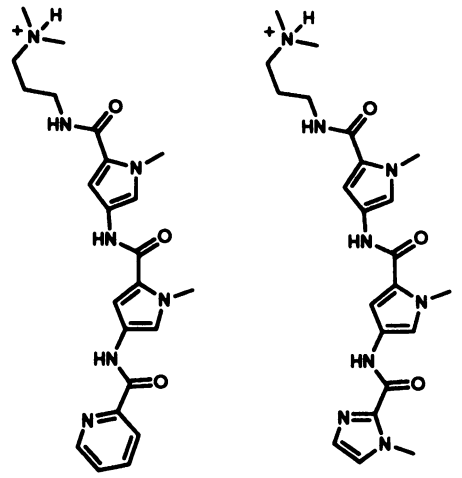

2-PyN 2-ImN

Although the x-ray structure of distamycin bound to the sequence 5′-AAATTT-3′ reveals a 1:1 complex (6), recent NMR studies indicate that at high concentration (2.0–4.0 mM), distamycin is also capable of binding A+T-rich DNA to form a 2:1 complex (21, 22). Such a 2:1 complex would explain the affinity cleavage data and the sequence specificity of 2-PyN and 2-ImN (19, 20). We describe here direct structural studies by NMR spectroscopy on the complex formed upon binding of 2-ImN to the oligonucleotide duplex d(GCATGACTCGG)·d(CCGAGTCATGC).

MATERIALS AND METHODS

Synthesis of 2-ImN. 2-ImN was prepared from *N*-methyl-4-(*N*-methyl-4-nitropyrrole-2-carboxamide)pyrrole-2-carboxylic acid (23) in four steps. Full synthetic details will be published elsewhere (20).

Sequence Specificity of 2-ImN. The binding of 2-ImN was compared with the distamycin analog, tris-*N*-methylpyrrolecarboxamide (P3) (3), on the 517-base-pair *Eco*RI/*Rsa* I

The publication costs of this article were defrayed in part by page charge payment. This article must therefore be hereby marked "*advertisement*" in accordance with 18 U.S.C. §1734 solely to indicate this fact.

Abbreviations: 2-PyN, pyridine-2-carboxamide netropsin; 2-ImN, 1-methylimidazole-2-carboxamide netropsin; NOESY, nuclear Overhauser effect spectroscopy.

restriction fragment of plasmid pBR322 by footprinting and affinity cleaving analyses. From footprinting analysis, at 2 μM concentration, the distamycin analog P3 binds to the 5-base-pair sites, in the following order of decreasing affinity: 5'-TTTTT-3' > 5'-AATAA-3' > 5'-TTAAT-3' >> 5'-TGTCA-3'. 2-ImN (at 10 μM concentration) was found to bind the 5-base-pair sites in the following order of decreasing affinity: 5'-TGTCA-3' >> 5'-TTTTT-'3 > 5'-AATAA-3' $\approx$ 5'-TTAAT-3'. Affinity cleaving experiments with 2-ImN-EDTA·Fe reveals that the synthetic peptide binds in two equivalent orientations to the 5'-TGTCA-3' site (20).

Sample Preparation. NMR samples were prepared by dissolving the undecamer in 0.25 ml of 20 mM sodium phosphate buffer (pH 7.0) and then lyophilizing to dryness. For experiments carried out in ^2H_2O, the solid was lyophilized twice from 99.9% ^2H_2O (Cambridge Isotope Laboratories, Cambridge, MA) and finally redissolved in 0.5 ml of 99.99% ^2H_2O (Cambridge Isotope Laboratories). For experiments in H_2O, the solid was redissolved in 90% H_2O and 10% ^2H_2O to a final vol of 0.5 ml.

A stock solution of 2-ImN·HCl was prepared by dissolving 2.5 mg of the ligand in 150 μl of 99.99% ^2H_2O containing 10 mM sodium phosphate buffer (pH 7.0). The concentration of the stock solution was determined to be 32 mM by UV absorbance at 302 nm ($\varepsilon = 3.5 \times 10^4$ $M^{-1}\cdot cm^{-1}$). Extinction coefficients for d(GCATGACTCGG) and d(CCGAGTCATGC) were calculated to be 1.05×10^5 $M^{-1}\cdot cm^{-1}$ and 1.02×10^5 $M^{-1}\cdot cm^{-1}$, respectively (24). The concentration of the double-stranded DNA sample was determined to be 2 mM by UV absorbance at 260 nm at 80°C.

One-Dimensional NMR Titration. 2-ImN·HCl was titrated into the NMR sample containing the DNA in 0.25 mol equivalents per addition. One-dimensional spectra were acquired at 25°C by using 4096 complex points, 128 scans, and a spectral width of 6024 Hz. A presaturation pulse was applied during the 2.0-sec recycle delay to suppress the residual $^1H^2HO$ resonance.

Two-Dimensional Nuclear Overhauser Effect Spectroscopy (NOESY) Spectra. NOESY spectra in ^2H_2O were acquired at 15°C using the standard time-proportional phase incrementation (TPPI) pulse sequence (25). The spectra were collected with 1024 complex points in t_2 using a spectral width of 5000 Hz (500 MHz) or 6024 Hz (600 MHz) and a mixing time of 200 msec. Typically, 512 t_1 experiments were recorded and zero-filled to 1 K. For each t_1 value 64 scans were signal averaged using a recycle delay of 2 sec. A presaturation pulse was applied during the recycle and mixing periods to suppress the residual $^1H^2HO$ resonance.

NOESY spectra in water were acquired at 15°C, replacing the last 90° pulse by 1:1 to suppress the solvent signal, using the pulse sequence delay -90°_x-t_1-90°_{-x}-τ_{mix}-90°_x-Δ^{11}-90°_ϕ-t_2 (26). Phase-sensitive detection was accomplished with TPPI. The spectra were collected with 2048 complex points in t_2 with a spectral width of 13,514 Hz and mixing times of 100 and 200 msec. Typically, 547–567 t_1 experiments were recorded and zero-filled to 2 K. The delay period Δ^{11} was calibrated to give optimum excitation in the imino region of the ^1H spectrum (11–13 ppm) with a single null at the water resonance.

The data were processed with FTNMR software (Hare Research, Woodinville, WA) on a Vax 11/785 computer or with FELIX software (Hare Research) on a Silicon Graphics IRIS/4D workstation. The two-dimensional NOESY data were apodized with a skewed sine bell function in both dimensions (800–1600 points, phase 60°, skew 0.5 in t_2; 512–567 points, phase 60°, skew 0.7 in t_1). The first row of the data matrix was multiplied by 0.5 prior to Fourier transformation in t_1 to suppress t_1 ridges.

Distance Constraints. Intermolecular distance constraints were generated from the volume integrals of the crosspeaks in the H_2O NOESY spectra acquired at mixing times of 100 and 200 msec. Volume integrals were measured for each mixing time using FELIX software. The crosspeak volumes were scaled according to $V_{corr} = V_{obs}/\sin(\Delta\omega\cdot\tau)$, where V_{corr} is the corrected crosspeak volume, V_{obs} is the measured crosspeak volume, τ is the delay adjusted to optimize excitation of the region of interest, and $\Delta\omega$ is the difference in frequency between the null and the crosspeak of interest in F2. The crosspeak volumes were classified semiquantitatively into three categories: strong (<2.5 Å), medium (between 2.5 and 3.7 Å), or weak (>3.7 Å) relative to the volume integrals of the cytosine H5–H6 crosspeak volumes at each mixing time. In all, 34 intermolecular ligand–DNA constraints and 5 intermolecular ligand–ligand constraints were used.

Structure Refinement. The initial structure for refinement calculations was a duplex of sequence d(GCATGACTCGG)·d(CCGAGTCATGC) constructed using the Biopolymer module of InsightII (Biosym Technologies, San Diego) with standard B-DNA helical parameters. For the ligands, the coordinates for the two distamycin molecules in the energy minimized NMR structure of the 2:1 complex with d(CGCAAATTGGC)·d(GCCAATTTGCG) (21) were read into InsightII. Using the Builder module of InsightII, the distamycin molecules were transformed into 2-ImN molecules. The Silicon Graphics workstation facilitated a simple docking procedure to produce the starting coordinates for the ligand dimer–DNA complex. Energy minimizations were performed by using the Discover module of InsightII. NOE distance constraints were incorporated into the structure prior to each simulation. A cutoff distance of 15 Å was used for nonbonded interactions and the neighbor list was regenerated every 20 time steps. A distance-dependent dielectric of the form $\varepsilon = R$ was used to account for solvent effects. The energy of the complex was minimized initially by using 100 steps of a steepest descent algorithm and further by using 15,000 steps of conjugate gradient minimization with an NMR force constant of 50 (kcal/mol)/Å to an rms derivative of <0.01 (kcal/mol)/Å.

RESULTS

Titration of 2-ImN. The results of the titration of 2-ImN into an NMR sample of the duplex d(GCATGACTCGG)·d(CCGAGTCATGC) are shown in Fig. 1. The individual aromatic base protons of the central 3-base-pair site in the free duplex are indicated by stars. These were assigned in the NOESY spectrum of the free duplex by standard sequential methods (27). Upon addition of substoichiometric amounts of 2-ImN, the NMR spectrum increases in complexity as evidenced by a doubling of the number of resonances. At a ligand/DNA ratio of 0.5:1, new resonances appear (squares) whose intensities are one-third the intensity of the free DNA signals. At a ligand/DNA stoichiometry of 1:1, the ratio of signal intensities of complexed DNA to free DNA is 1:1, indicating that one-half of the DNA exists as complex. Subsequent additions of 2-ImN to the sample act solely to increase the intensities of the signals from complexed DNA as well as the signals from bound ligand. At a ligand/DNA ratio of 2:1 only one set of DNA resonances and one set of bound ligand resonances are present, implying that a single ligand–DNA complex has been formed. Furthermore, a comparison of the peak intensities of complexed to free DNA as a function of increasing concentration of ligand shows that this single complex has a stoichiometry of 2:1. The sharpness of the ligand and DNA signals throughout the titration indicates that the ligands are in slow exchange on the NMR time scale.

Signal Assignments. Two-dimensional NOESY spectra of the complex in ^2H_2O were acquired at two equivalents of

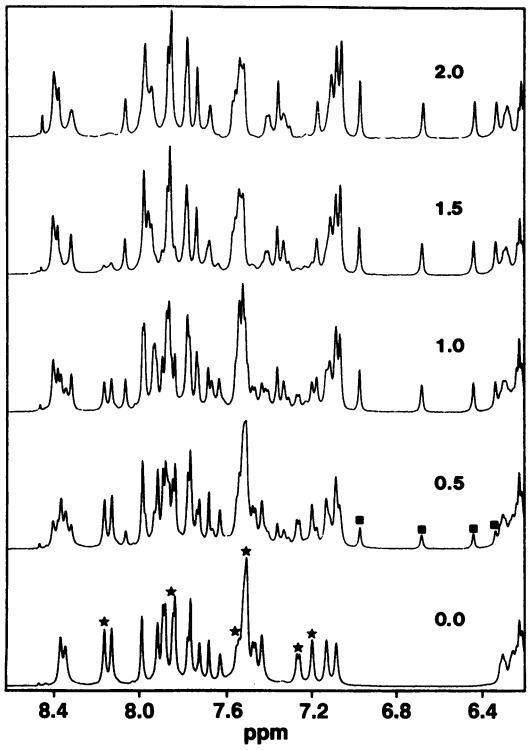

FIG. 1. Aromatic region of NMR spectra acquired at several points in a titration of d(GCATGACTCGG)·d(CCGAGTCATGC) with 2-ImN at 25°C.

added ligand. Each aromatic base proton (H8 of purines, H6 of pyrimidines) was assigned through its connectivity to C1'H of its own sugar and the C1'H of its 5' neighbor. Assignment of the imino protons in the H_2O NOESY by standard methods (28) facilitated the assignment of the adenine C2H protons in the complex. The amino NH_2 protons of G5 and G16 were assigned via their connectivities to ligand pyrrole H3 and imidazole H4 protons. Ligand amide NH protons, pyrrole H3, and imidazole H4 protons were assigned by intramolecular connectivities among these protons in the NOESY spectrum of the complex in H_2O. Ligand methylene protons (C18) were assigned via intermolecular contacts to the imidazole H4 proton on the opposite ligand of the 2:1 complex.

Intermolecular Contacts. The NOESY spectrum of the 2:1 complex in H_2O is shown in Fig. 2. The spectrum contains numerous intermolecular contacts that enable the placement of the ligands on the DNA. The ligand–ligand and ligand–DNA contacts are summarized in Table 1. Strong NOE crosspeaks between the imidazole H4 protons and the NH_2 protons of G5 and G16, as well as between the H3-2 and H3-3 pyrrole protons of both ligands and the C2H protons of A6 define the orientations of the ligands. The ligands stack on top of one another in an antiparallel fashion. These intermolecular contacts are shown schematically in Fig. 3. Further contacts between ligand amide protons and DNA protons along the minor groove of the central 5-base-pair binding site confirm the placement of the ligands. The relative position of the ligands with respect to one another is also confirmed by five intermolecular ligand–ligand contacts.

Molecular Modeling. The intermolecular contacts listed in Table 1 plus ligand intramolecular contacts were used as constraints in the energy minimization procedure. The resulting structure is presented in Fig. 4. The charged end of each 2-ImN molecule lies deep in the minor groove, providing favorable contributions to the total free energy of the structure. For ligand 1, putative hydrogen bonds are formed between NH-1 and N3 of A6, NH-2 and O2 of C7, NH-3 and O2 of T8, and between N3 of the imidazole and the NH_2 group of G5. Analogous hydrogen bonds are found for ligand 2, with the imidazole N3 hydrogen-bonded to the NH_2 group of G16.

The stacking of the ligand molecules with respect to one another, as found by molecular modeling, is similar to the staggered antiparallel arrangement found in the 2:1 complex formed between distamycin and d(CGCAAATTGGC)·d(GCCAATTTGCG) (21).

DISCUSSION

Titration of the duplex d(GCATGACTCGG)·d(CCGAGTCATGC) with 2-ImN yields only one set of new resonances in the one-dimensional NMR spectrum. Analysis of two-dimensional NMR spectra reveals that these resonances are associated with a 2:1 ligand–DNA complex. Thus, even at low ligand/DNA stoichiometries (e.g., 0.25:1) dimeric binding is dominant, indicating that the two ligands bind with high cooperativity. In contrast, studies of the complexes formed between distamycin and the 5'-AAATT-3' and 5'-AAATTT-3' duplexes do not show evidence for the 2:1 binding mode until 0.5–0.75 equivalent of ligand has been added (21, 22). Replacement of A·T base pairs with inosine·cytosine (I·C) base pairs, which present the same functional groups on their minor groove surfaces, affords highly cooperative dimeric binding of distamycin to the sequence d(CGCIIICCGGC)·d(GCCIICCCGCG) (29). If G·C- or I·C-bearing DNA sequences have inherently wider minor grooves, formation of 2:1 complexes on ligand binding may be favored as a result of a reduction in the energy cost to accommodate the second ligand. In addition, single ligand binding modes for such sequences would be disfavored if their grooves were not capable of clamping down sufficiently on one ligand to maximize the van der Waals contacts necessary for binding.

The ligand binding sites of the 2-ImN complex are defined by the intermolecular ligand–DNA NOEs given in Table 1. For ligand 1, the pyrrole protons H3-2 and H3-3 give strong NOEs to C2H of A6 and C1'H of C7, and NH_2 of G16 and C1'H of T8, respectively. The imidazole H4 proton of ligand 1 has a strong NOE to NH_2 of G5. Therefore, the imidazole–pyrrole–pyrrole ring system of ligand 1 spans the G5-A6-C7 sequence with the imidazole ring oriented to the 5' side of the strand. Likewise, for ligand 2, H3-2 and H3-3 pyrrole protons are proximal to C2H of A6 and C1'H of C18, and to NH_2 of G5 and C1'H of A19, respectively. The imidazole H4 proton of ligand 2 gives a strong NOE to NH_2 of G16. These data indicate that the imidazole–pyrrole–pyrrole ring system of ligand 2 spans the same G5-A6-C7 sequence as ligand 1, but in the opposite orientation. NOEs between CH2 of C18 on ligand 1 and imidazole H4 on ligand 2, as well as between CH2 of C18 on ligand 2 and imidazole H4 on ligand 1, confirm the orientations of the ligands on the DNA and relative to one another. These data indicate that the dimeric binding site is in the minor groove of the central portion of this DNA oligomer.

The stability of the 2-ImN–DNA complex is determined by several factors. The amide NH protons contribute favorably to the binding energy through hydrogen bond formation to thymine O2 and adenine N3 atoms. Pyrrole H3 protons and the imidazole H4 proton form close van der Waals contacts with sugar C1'H and adenine C2H protons of the DNA. The positively charged *N,N*-dimethylammonium group facilitates the attraction of the ligand to DNA. Stacking of the conjugated ring systems of the ligands in the 2:1 complex provides additional binding energy. Maximizing the contacts that provide the binding energy may require some distortion of the duplex and the concomitant energetic penalty. From the NMR studies presented here and chemical protection experiments, there is no strong evidence for major distortions of the DNA helix or conformation as a result of 2-ImN binding to 5'-TGACT-3' (19).

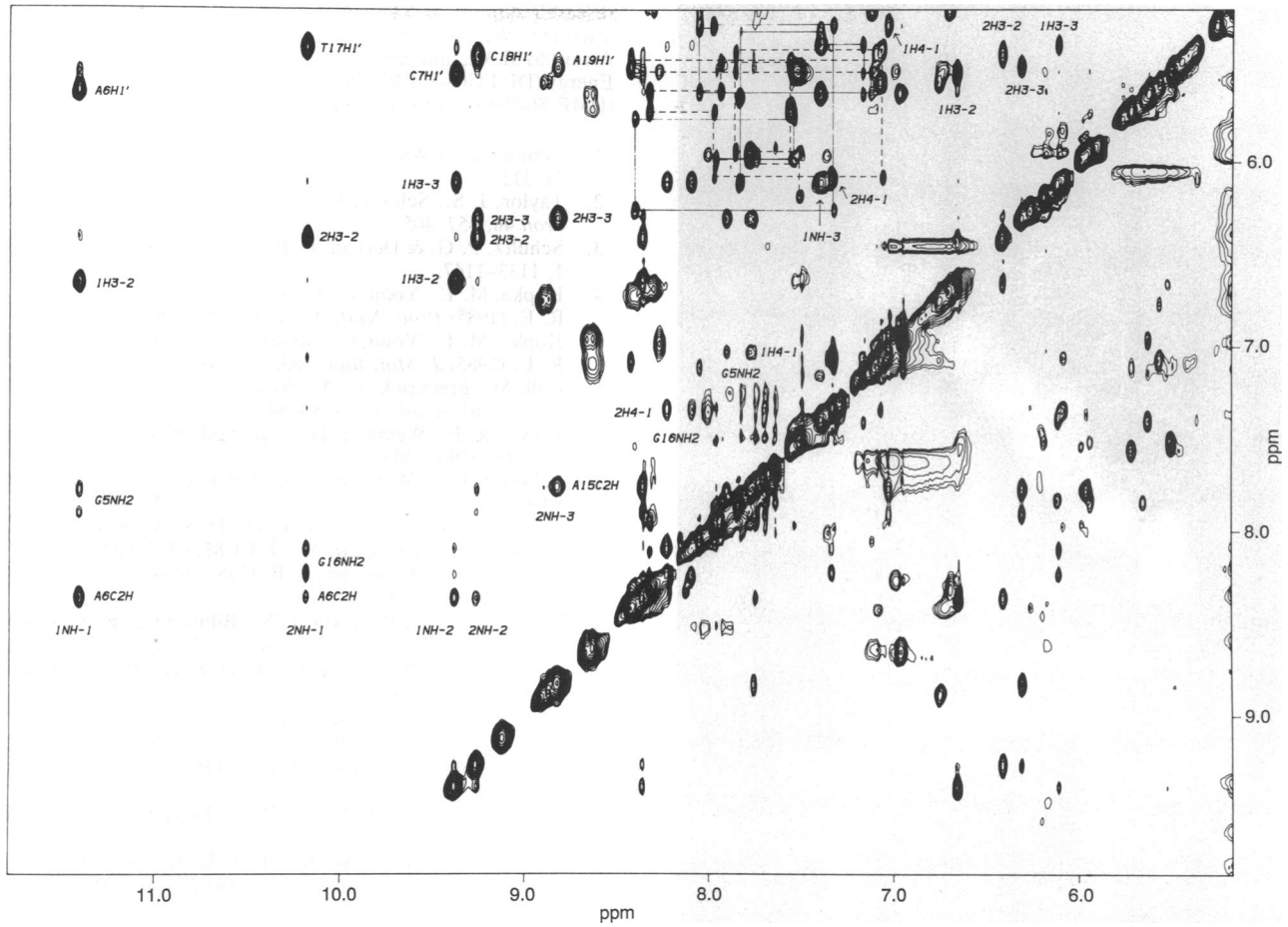

FIG. 2. Expansion of the aromatic and amide region of a NOESY spectrum of the 2:1 2-ImN–d(GCATGACTCGG)·d(CCGAGTCATGC) complex (in 90% H_2O/10% ^2H_2O; 15°C; mixing time, 200 msec). Sequential aromatic to C1′H connectivities for the 5′-TGACT-3′ strand are shown as solid lines; those for the 5′-AGTCA-3′ strand are shown as dashed lines. Crosspeaks are labeled according to their chemical shifts along ω_1 (vertical axis, label beside the peak) and along ω_2 (horizontal axis, label above or below the peak). Labeling conventions for ligands 1 and 2 are NH- for amide hydrogens, H3- for pyrrole hydrogens, and H4-1 for the imidazole hydrogen, numbered from the imidazole end to the ammonium end.

The most striking feature of the $(2\text{-ImN})_2$–5′-TGACT-3′ complex is the specific recognition of both G·C and A·T base pairs. Molecular modeling of the 2:1 complex suggests that the imidazole nitrogen (N3) proximal to the 2-amino group of guanine affords a hydrogen bond that contributes to the

Table 1. Ligand–DNA and ligand–ligand intermolecular contacts

Ligand 1	DNA	Ligand 2
	Ligand–DNA	
	A19 C2H	NH-3
	A19 C1′H	NH-3, H3-3
H4-1	G5 C1′H	
NH-1, H4-1	G5 NH_2	NH-2, H3-3
	C18 C1′H	NH-2, H3-2
	T17 C1′H	NH-2
NH-1	A6 C1′H	
NH-1, H3-2	A6 C2H	NH-2, H3-2
NH-2, H3-2	C7 C1′H	
NH-2, H3-3	G16 NH_2	NH-1, H4-1
	G16 C1′H	H4-1
H3-3	T8 C1′H	
	Ligand–ligand	
C(18)H		H4-1
H3-2		H3-2
H4-1		C(18)H
NH1		H3-2
H3-2		NH-2

Contacts were identified in the H_2O NOESY acquired at 200 msec mixing time.

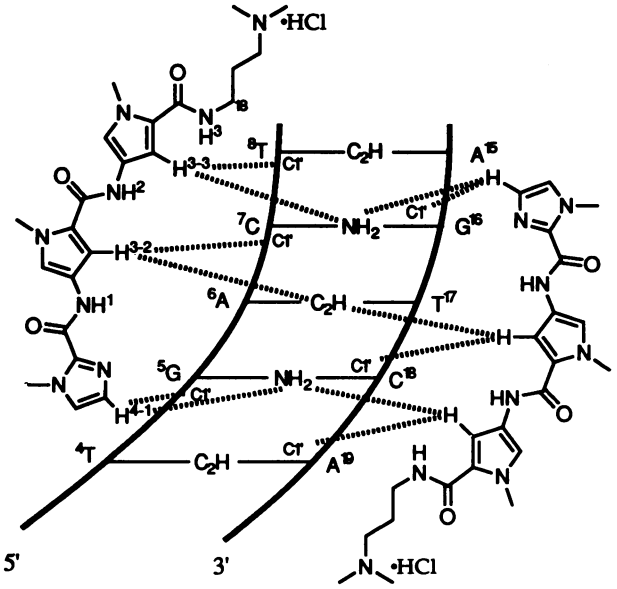

FIG. 3. Schematic of selected intermolecular NOEs between 2-ImN and d(GCATGACTCGG)·d(CCGAGTCATGC).

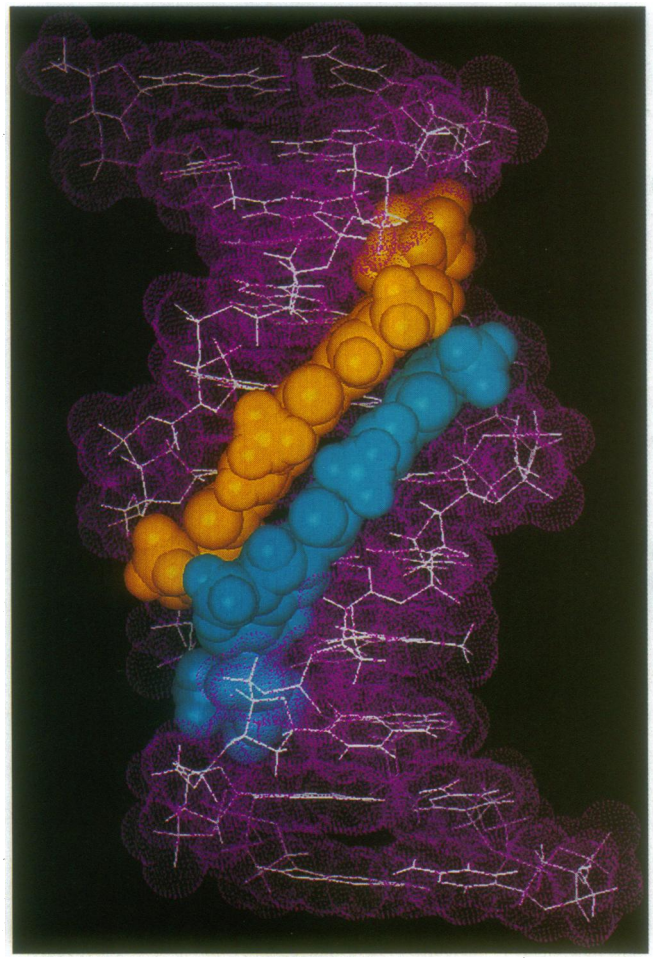

FIG. 4. van der Waals surface representation of the 2-ImN–d(GCATGACTCGG)·d(CCGAGTCATGC) complex obtained by energy refinement using semiquantitative distance constraints derived from NOESY.

stability of the complex. There may be an energetic price for this recognition if the crescent-shaped 2-ImN does not sit deeply in the minor groove of the sequence 5′-TGACT-3′.

Undoubtedly, this antiparallel side-by-side 2:1 peptide–DNA complex broadens the structural repertoire beyond 1:1 complexes for design considerations of sequence-specific minor groove binding molecules. The generality of this motif for the sequence-specific recognition of a large number of DNA sequences remains to be seen. We are encouraged by the recent simultaneous finding that a different distamycin analog containing a central imidazole binds the sequence 5′-AAGTT-3′ as a 2:1 complex (30). Dimeric motifs seem unlikely to be limited to *N*-methylpyrrole-carboxamide analogs. We note that chromomycin, an oligosaccharide chromophore, binds in the minor groove as a 2:1 complex (31). Perhaps additional classes of side-by-side binders can be constructed that will act as shape-selective calipers for sequence-dependent minor groove width.

We are grateful to the National Institutes of Health (GM-27681 to P.B.D. and GM-43129 to D.E.W.) and Burroughs Wellcome for research support, a National Science Foundation predoctoral fellowship to W.S.W., a National Institutes of Health Research Service Award to M.M., and instrument grants from the U.S. Department of Energy (DE FG05-86ER75281) and the National Science Foundation (DMB 86-09305 and BBS 87-20134).

1. Zimmer, C. & Wähnert, U. (1986) *Prog. Biophys. Mol. Biol.* **47,** 31–112.
2. Taylor, J. S., Schultz, P. G. & Dervan, P. B. (1984) *Tetrahedron* **40,** 457–465.
3. Schultz, P. G. & Dervan, P. B. (1984) *J. Biomol. Struct. Dyn.* **1,** 1133–1147.
4. Kopka, M. L., Yoon, C., Goodsell, D., Pjura, P. & Dickerson, R. E. (1985) *Proc. Natl. Acad. Sci. USA* **82,** 1376–1380.
5. Kopka, M. L., Yoon, C., Goodsell, D., Pjura, P. & Dickerson, R. E. (1985) *J. Mol. Biol.* **183,** 553–563.
6. Coll, M., Frederick, C. A., Wang, A. H.-J. & Rich, A. (1987) *Proc. Natl. Acad. Sci. USA* **84,** 8385–8389.
7. Klevit, R. E., Wemmer, D. E. & Reid, B. R. (1986) *Biochemistry* **25,** 3296–3303.
8. Pelton, J. G. & Wemmer, D. E. (1988) *Biochemistry* **27,** 8088–8096.
9. Yoon, C., Prive, G. G., Goodsell, D. S. & Dickerson, R. E. (1988) *Proc. Natl. Acad. Sci. USA* **85,** 6332–6336.
10. Schultz, P. G. & Dervan, P. B. (1983) *Proc. Natl. Acad. Sci. USA* **80,** 6834–6837.
11. Skamrov, A. V., Rybalkin, I. N., Bibilashvili, R. S., Gottikh, B. P., Grokhovskii, S. L., Gurskii, G. V., Zhuze, A. L., Zasedatelev, A. S., Nechipurenko, Y. D. & Khorlin, A. A. (1985) *Mol. Biol.* **19,** 153–167.
12. Youngquist, R. S. & Dervan, P. B. (1985) *Proc. Natl. Acad. Sci. USA* **82,** 2565–2569.
13. Youngquist, R. S. & Dervan, P. B. (1985) *J. Am. Chem. Soc.* **107,** 5528–5529.
14. Youngquist, R. S. & Dervan, P. B. (1987) *J. Am. Chem. Soc.* **109,** 7564–7566.
15. Lown, J. W., Krowicki, K., Bhat, U. G., Skorobogaty, A., Ward, B. & Dabrowiak, J. C. (1986) *Biochemistry* **25,** 7408–7416.
16. Kissinger, K., Krowicki, K., Dabrowiak, J. C. & Lown, J. W. (1987) *Biochemistry* **26,** 5590–5595.
17. Lee, M., Chang, D. K., Hartley, J. A., Pon, R. T., Krowicki, K. & Lown, J. W. (1988) *Biochemistry* **27,** 445–455.
18. Wade, W. S. & Dervan, P. B. (1987) *J. Am. Chem. Soc.* **109,** 1574–1575.
19. Wade, W. S. (1989) Ph.D. thesis (California Inst. of Technology, Pasadena).
20. Wade, W. S., Mrksich, M. & Dervan, P. B. (1992) *J. Am. Chem. Soc.*, in press.
21. Pelton, J. G. & Wemmer, D. E. (1989) *Proc. Natl. Acad. Sci. USA* **86,** 5723–5727.
22. Pelton, J. G. & Wemmer, D. E. (1990) *J. Am. Chem. Soc.* **112,** 1393–1399.
23. Lown, J. W. & Krowicki, K. (1985) *J. Org. Chem.* **50,** 3774–3779.
24. Warshaw, M. & Cantor, C. (1970) *Biopolymers* **9,** 1079–1103.
25. Drobny, G., Pines, A., Sinton, S., Weitekamp, D. P. & Wemmer, D. E. (1979) *Faraday Div. Chem. Soc. Symp.* **13,** 49–55.
26. Sklenar, V., Brooks, B. R., Zon, G. & Bax, A. (1987) *FEBS Lett.* **216,** 249–252.
27. Hare, D. R., Wemmer, D. E., Chou, S.-H., Drobny, G. & Reid, B. R. (1983) *J. Mol. Biol.* **171,** 319–336.
28. Wuthrich, K. (1986) *NMR of Proteins and Nucleic Acids* (Wiley, New York).
29. Fagan, P. A. & Wemmer, D. E. (1992) *J. Am. Chem. Soc.* **114,** 1080–1081.
30. Dwyer, T. J., Geierstanger, B. H., Bathini, Y., Lown, J. W. & Wemmer, D. E. (1992) *J. Am. Chem. Soc.*, in press.
31. Gao, X. & Patel, D. J. (1989) *Biochemistry* **28,** 751–762.